

# INTEGRAL SLIDING-MODE CONTROL OF A PIEZOELECTRIC-ACTUATED MOTION STAGE

Jing-Chung Shen, Wen-Yuh Jywe, \*Chien-Hung Liu  
\*\*Yu-Te Jian, \*\*\*Yun-Feng Deng and \*\*\*\*Yue-Tzu Yang

*Department of Automation Engineering  
National Formosa University  
Huwei, Yunlin, Taiwan  
Email: jcshen@nhust.edu.tw*

*\*Department of Electro-Optic Engineering  
National Formosa University  
Huwei, Yunlin, Taiwan*

*\*\*Institute of Mechanic and Mechatronic Engineering  
National Formosa University  
Huwei, Yunlin, Taiwan*

*\*\*\*Department of Mechanical Engineering  
National Chung Cheng University  
Chiayi, Taiwan*

*\*\*\*\*Department of Mechanical Engineering  
National Cheng Kung University  
Tainan, Taiwan*

**Abstract:** This paper presents the design of an integral sliding-mode controller for a piezoelectric-actuated system. The sliding-mode disturbance (uncertainty) estimation and compensation scheme is used. The nonlinear piezoelectric-actuated system is modeled as a first order linear model coupled with a hysteresis. When the model is identified, the hysteresis nonlinearity is linearized then the linear system model with uncertainty is used to design the sliding-mode controller. The structure of the proposed controller is as simple as the PID controller. Thus, it can be implemented easily. This design method is applied to the motion control of a nano-stage and experimental results are presented. *Copyright © 2005 IFAC*

**Keywords:** Sliding-mode control, Hysteresis, Actuator, Precision, Nonlinear.

## 1. INTRODUCTION

Piezoelectric actuators are becoming increasingly important in today's positioning technology due to the requirements of nanometer resolution in displacement. It is well known that the piezoelectric actuator has many advantages (Hwang, *et al.*, 2003; Ku, *et al.*, 2000) such as: 1) there are no moving parts; 2) the actuators can produce large forces; 3) they have almost unlimited resolution; 4) the efficiency is high; and 5) response is fast. However, it also has some bad characteristics such as: 1) hysteresis behavior; 2) drift in time; 3) temperature dependence. Hysteresis characteristics are generally nondifferentiable nonlinearities and usually unknown, this often limits system

performance via, e.g., undesirable oscillations or instability. Therefore, it is difficult to obtain an accurate trajectory tracking control.

Recently, several methods have been reported for the trajectory tracking control of a piezoelectric-actuated system. These methods can be separated into two approaches: feedforward control (Ge and Jouaneh, 1996, 1997; Ku, *et al.*, 2000) and inverse control (Cruz-Hernandez and Hayward, 2001; Hwang and Lin, 2004; tao and Kokotovic, 1995; Xu, 1993; Hwang, *et al.*, 2001, 2003). Ge and Jouaneh (1996, 1997) used a combination of a proportional integral derivative (PID) feedback controller with a feedforward controller that included the Preisach model of hysteresis. Their experimental results

showed that the tracking performance was improved greatly. However, the result in (1996) is only valid for a sinusoidal trajectory and the method in (1997) needs to train the model by using reference input before the control started. Ku *et al.* (2000) combined a PID feedback controller with an adaptive neural network feedforward controller to control a nanopositioner that was actuated by a piezoelectric actuator.

In the inverse control approach, Cruz-Hernandez and Hayward (2001) proposed a variable phase method. They utilized an operator to shift the periodic input signal by a phase angle that depended on the amplitude of the input signal, then used this operator to reduce the hysteresis nonlinearity. Huang and Lin (2004) proposed a new hysteresis model based on two first-order transfer functions in parallel with two parameters determined from experiment. Adaptive control is also an approach to the inverse control of plants with hysteresis behavior. Tao and Kokotovic (1995) developed an adaptive hysteresis inverse and cascaded it with the system so that the effects of hysteresis nonlinearity could be reduced. Xu (1993) utilized an adaptive neural network inverse controller to compensate the hysteretic behavior of a piezoelectric actuator and a PI controller in the outer loop to overcome the remaining nonlinear uncertainty. Furthermore, Hwang *et al.* (2001) utilized an offline learned neural network model to reduce the effect of hysteresis then designed a discrete-time variable structure controller to overcome the remaining uncertainty. They also reinforced this method (Hwang, *et al.*, 2003) by using a recurrent neural network to improve the control performance. However, the computation burden of the controller that was designed by their method is heavy.

In this paper, an integral sliding-mode controller for a piezoelectric-actuated system is presented. Firstly, the piezoelectric-actuated system was modeled as a first order uncertain linear model coupled with a hysteresis nonlinearity. Then the hysteresis nonlinearity was linearized and the resulting uncertain linear model was used to design the sliding-mode controller. In this study, the sliding-mode uncertainty (disturbance) estimation and compensation scheme (Utkin, 1999; Shen, 2000) is used. Since the model of the system is first order, the structure of the proposed controller is as simple as the PID controller. Therefore, it can be implemented easily. Finally, this design method was applied to the motion control of a nano-stage. The experimental results are presented that verify the usefulness of this method.

## 2. SYSTEM MODELING AND CONTROLLER DESIGN

### 2.1 System model

When the step response of a piezoelectric-actuated system is essentially monotone (Hagglund *et al.*, 2002), it can be modeled by a first order uncertain linear system coupled with a hysteresis nonlinearity as shown in Fig. 1. Where  $u$  is the input,  $H$  describes the hysteresis behavior of the piezoelectric actuator,  $d$  represents the disturbance and the first order differential equation

$$T(1 + \Delta(t))\dot{x} + x = v, \quad (1)$$

describes the dynamic behavior of the system. Where  $T$  is the nominal time constant and  $\Delta(t)$  represents the uncertainty. Parameter  $T$  and the bound of  $\Delta(t)$  can be determined by doing step response tests at various working points.

From Fig. 1,  $v$  can be represented as

$$v = Ku + N(t) + d(t), \quad (2)$$

where  $K$  is the linearized gain of the hysteresis and  $N(t)$  represents the nonlinear uncertain part of the hysteresis. From (1) and (2), the following dynamic equation can be obtained:

$$\dot{x} = -\frac{x}{T} + \frac{Ku}{T} + \phi(t) \quad (3)$$

where

$$\phi(t) = \frac{\Delta(x - Ku) + N + d}{T(1 + \Delta)}$$

represents the disturbance and uncertainties.

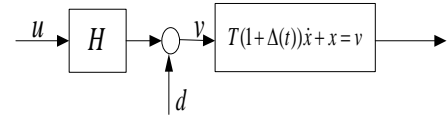


Fig. 1. Model of the piezoelectric-actuated system.

### 2.2 Sliding-mode controller design

This subsection describes how to design the sliding mode controller. In this study, the sliding mode disturbance (uncertainty) estimation and compensation scheme is applied to design the closed-loop controller for the piezoelectric-actuated system.

Let  $x_d$  be the desired displacement, which may be time varying. Define

$$e = x_d - x \quad (4)$$

as the tracking error. From (3) and (4), the error dynamics can be obtained as

$$\dot{e} = \dot{x}_d - \dot{x} = \dot{x}_d + \frac{x}{T} - \frac{K}{T}u - \phi(t). \quad (5)$$

Let the control law be

$$u = \frac{x}{K} + \frac{T}{K}(\lambda e + \dot{x}_d) + u_d \quad (6)$$

where  $\lambda$  is the feedback gain to be designed so that the error dynamic will have the desired response while the system is free of disturbance and uncertainty, and  $u_d$  is the uncertainty and the disturbance compensation component yet to be determined by the sliding mode estimator.

Defining the switching function as

$$S = z - e \quad (7)$$

with

$$\dot{z} = -\lambda e - \frac{K}{T} u_d + \psi, \quad z(0) = e(0) \quad (8)$$

where  $z$  is the state variable of this auxiliary process,  $\psi$  is the switching action assigned as

$$\psi = -\eta \text{sign}(S),$$

$$\text{sign}(S) = \begin{cases} 1 & \text{if } S > 0 \\ -1 & \text{if } S < 0 \\ 0 & \text{if } S = 0 \end{cases} \quad (9)$$

and the positive constant  $\eta$  satisfies

$$\eta > |\dot{\phi}(t)| \quad (10)$$

Ensuring a sliding regime  $S = 0$  requires consideration of the Lyapunov candidate  $V = 0.5S^2$ . Differentiating  $V$  with respect to time and substituting (5-8) to obtain

$$\dot{V} = S(\dot{z} - \dot{e}) = S[(-\eta \text{sign}(S) + \dot{\phi}(t))] \quad (11)$$

From (10) and (11), it is seen that

$$\dot{V} < 0 \quad \text{if } S \neq 0 \quad (12)$$

Thus the sliding condition is satisfied. Note that  $z(0) = e(0)$ , therefore

$$S = 0 \quad \text{for } t = 0 \quad (13)$$

From (12) and (13), it can be concluded that the sliding mode exists at all times, *i.e.*,

$$S = 0 \quad \text{for all } t \geq 0 \quad (14)$$

Denote the equivalent value of  $\psi$  as  $\psi_{eq}$ . Since  $S = 0$ ,  $\psi_{eq}$  can be determined from (5), (7) and (8):

$$\psi_{eq} = -\dot{\phi} \quad (15)$$

This means that the equivalent value of  $\psi$  equals the uncertainties and disturbances. By selecting  $u_d = \frac{T}{K} \psi_{eq}$ , the uncertainties and disturbances can be compensated. It was shown in (Utkin, 1999) that the equivalent  $\psi_{eq}$  is equal to the average value measured by a first-order linear filter with the switched action as its input. Therefore,  $u_d$  can be written as

$$u_d = \frac{T}{K} \psi_{av} = \frac{T}{K} \psi_{eq} \quad (16)$$

with

$$\tau \dot{\psi}_{av} + \psi_{av} = \psi. \quad (17)$$

The time constant  $\tau$  should be made small enough that the plant and disturbance dynamics are allowed to pass through the filter without significant phase delay. Substituting (16) and (6) into (5) yields

$$\dot{e} + \lambda e = -\psi_{eq} - \dot{\phi},$$

which is equivalent to  $\dot{e} + \lambda e = 0$ . This equation represents the desired error dynamics.

### 3. EXPERIMENTAL RESULTS

#### 3.1 Experiment apparatus

In order to examine the performance of the controller described in the last section, this design method was used to control the motion (X, Y plane) of a multi-axis nano-stage. The structure of this nano-stage is shown in Fig. 2. Actuation of this nano-stage is done with a piezoelectric actuator (PSt1000/10/60 Vs18, Piezomechanik GmbH) with a nominal expansion of  $50 \mu\text{m}$  (at 1000V). Capacitance-type gap sensors (D-050, Piezomechanik GmbH) are used for position measurement. The total ranges of the gap sensors are  $50 \mu\text{m}$  with a sensitivity of  $0.2 \text{V} / \mu\text{m}$ . Control of this nano-stage is done with a controller board with a Power PC central processing unit (DS1103, dSPACE GmbH). The sampling rate of the control algorithm was 10 KHz. The resolution of A/D converters is 16-bit.

#### 3.2 Open-loop characteristics

In order to design a proper controller, it is necessary to understand the open-loop characteristics of this nano-stage. Firstly, the maximum moving range and hysteresis nonlinearity of the X and Y axes are tested. Fig. 3 shows the test result of the X-axis. The moving range of the X-axis and Y-axis is about  $32.5 \mu\text{m}$  and  $30 \mu\text{m}$  respectively. From the figure, the linearized gain of the X and Y axes can be obtained as  $0.04 \mu\text{m}/\text{V}$  and  $0.0344 \mu\text{m}/\text{V}$  respectively.

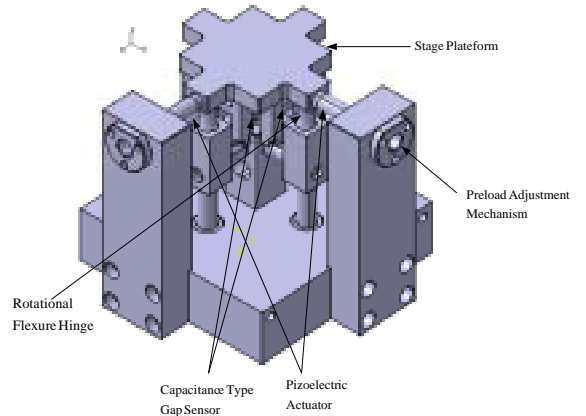


Fig. 2. Structure of the multi-axis nano-stage.

In order to identify the nominal time constant  $T$  and estimate the bound of  $\Delta$ , step response tests at various working points of the X and Y axes are executed. One of the test results is shown in Fig. 4. From the test results, it was found that the time constant of the X-axis (Y-axis) lies between 5 and 13 (5 and 15) mini seconds. Finally, the frequency-response experiments for the X and Y axes are conducted. When measuring the frequency response, a bias voltage was added to push the stage platform to the center of the moving range. Then, a random excitation signal was sent to the piezoelectric actuator and the displacement of the X and Y axes is measured by the gap sensor. The test results are depicted in Fig. 5. As seen in Fig.5, there are resonances at about 1.1, 1.4 and 1.75 kHz, the bandwidth of the X-axis and Y-axis are about 100 Hz and 95 Hz respectively and the coupling effects on the X and Y axes are less than 10% in magnitude up to the 1-kHz frequency range.

### 3.3 Control results

In this study, the coupling effects are treated as disturbances and the controllers for the X and Y axes are designed independently. When designing the controller,  $\lambda$  is chosen as large as possible to obtain wider bandwidth. The final controller parameters for the X-axis are chosen as follows:  $\lambda = 550$ ,  $\eta = 5$  and  $\tau = 0.0018$ . While the parameters for the Y-axis are chosen as follows:  $\lambda = 600$ ,  $\eta = 5$  and  $\tau = 0.0018$ .

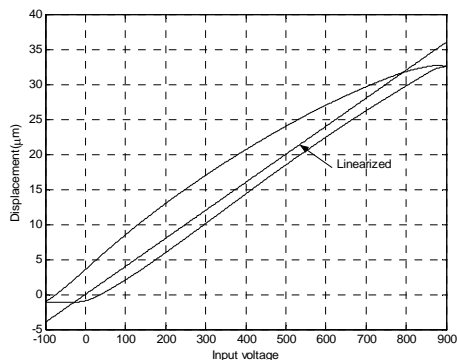


Fig. 3. Hysteresis nonlinearity of the X axis.

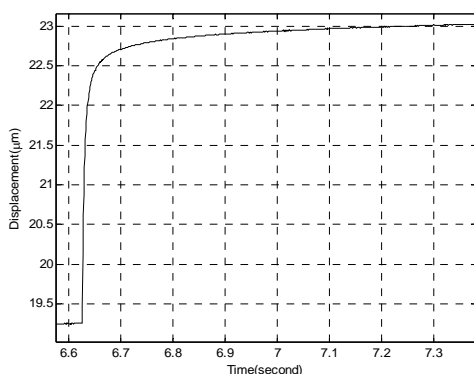
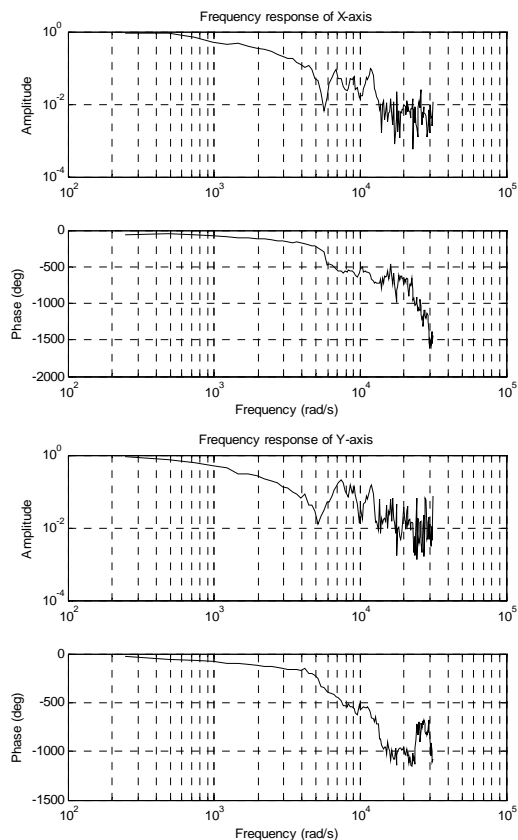
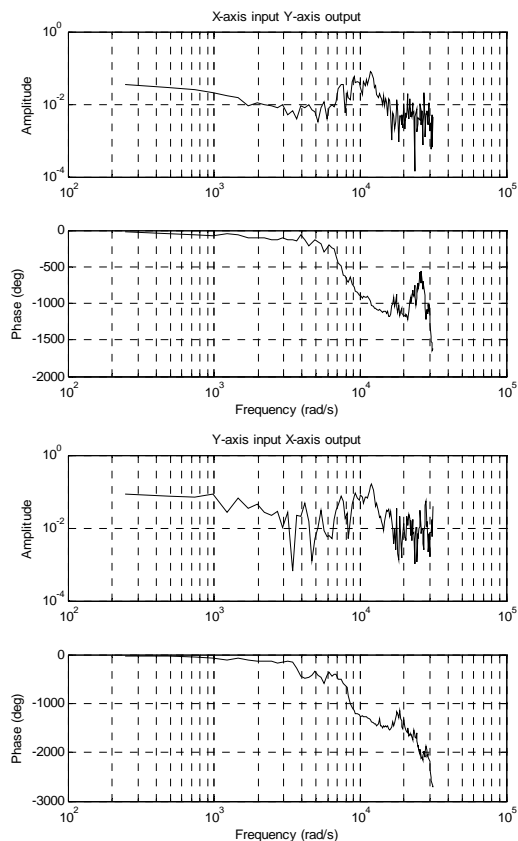


Fig. 4. Result of a step response test.



(a) Frequency response of X and Y axes.



(b) Frequency response of coupled motion.

Fig. 5. Frequency responses of the nano-stage.

The results of some experiments are shown in Figs. 6-9. Fig. 6 and Fig. 7 are the trajectory following results (X axis) of 3 Hz sine wave and triangle wave. It can be seen that the X axis can track the desired trajectory very well. The tracking error of the sine wave is below 3% of the maximum amplitude, while the tracking error of the triangle wave is about 5% of the maximum amplitude. In order to test the precision of the position control, the amplitude of sine wave was decreased to 5nm. Fig. 8 shows the response of the X-axis to this reference input. For a very small amplitude of reference position of 5nm which is almost the same as the magnitude of noise, the measured output still tracked the reference input fairly well. It can be concluded that tracking resolution is about 5nm. Fig.9 shows the result of tracking a circle (1 Hz) with  $4\ \mu\text{m}$  diameter. Fig. 10 shows the error analysis results. As the results show, the circular deviation is about  $15.6\ \text{nm}$ . From the results, it can be concluded that the disturbances and uncertainties can be estimated and then compensated.

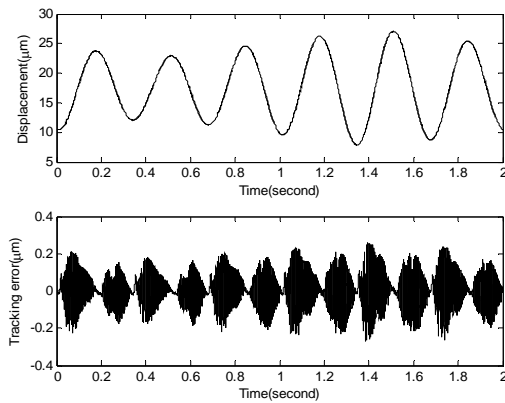


Fig. 6. Result of tracking a 3Hz sin wave with varying amplitude (X-axis).

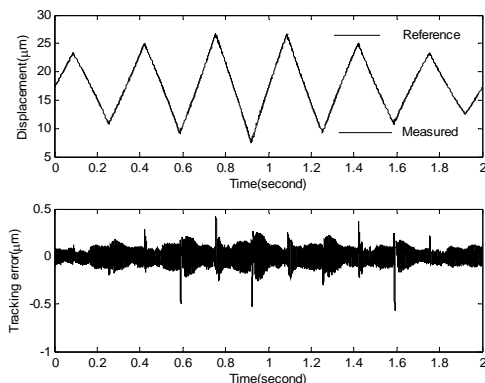


Fig. 7. Result of tracking a 3Hz triangle wave with varying amplitude (X-axis).

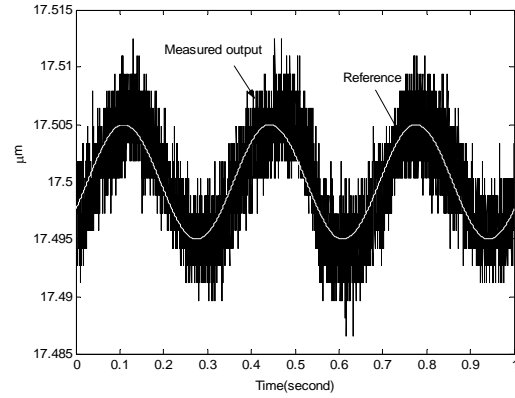


Fig. 8. Resolution of the X-axis.

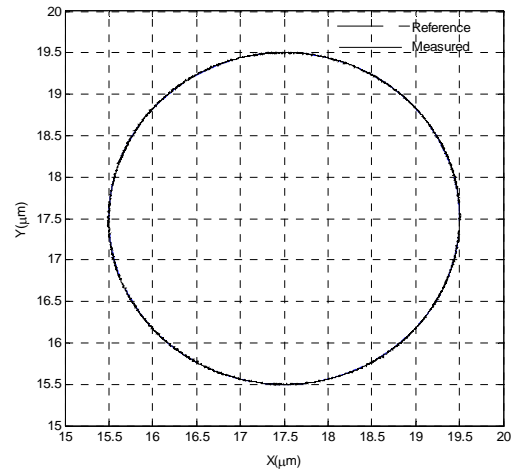
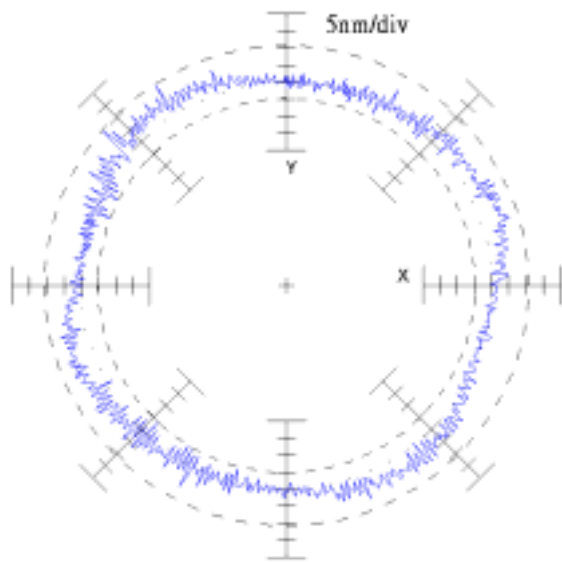


Fig. 9 Tracking response to a circle with  $4\ \mu\text{m}$  - diameter.

#### 4. CONCLUSIONS

This article proposed an integral sliding-mode controller design method for piezoelectric actuated systems. This method was then used to design the controllers for a nano-stage. Experiments on tracking the sinusoidal waveforms, triangle waveforms and circles were carried out. From the result it can be seen that the performance of this controller is good and 5nm tracking resolution can be obtained. Moreover, the result of circle tracking has shown that the controller designed by the proposed method can estimate the disturbance (uncertainty) and then compensate it. The most important feature is that the proposed controller is as simple as a PID controller. Therefore, it can be implemented easily.



Circular deviation:	0.0156 $\mu\text{m}$
Minimum radial deviation:	-0.0048 $\mu\text{m}$
Maximum radial deviation:	+0.0108 $\mu\text{m}$
Centre point comp. val.:	X:0.0000 $\mu\text{m}$ Y:0.0001 $\mu\text{m}$

Fig. 10. Error analysis results of circle tracking.

#### ACKNOWLEDGEMENTS

The authors want to thank the National Science Council of Taiwan for financial support provided under grant no. NSC92-2622-E-150-029.

#### REFERENCES

- Cruz-Hernandez J. and V. Hayward (2001). Phase Control Approach to Hysteresis Reduction. *IEEE Transaction on Control Systems Technology*, **9**, pp. 17-26.
- Ge P. and M. Jouaneh (1996). Tracking Control of a Piezoceramic Actuators. *IEEE Transactions on Control System Technology*, **4**, pp. 209-216.
- Ge P. and M. Jouaneh (1997). Generalized preisach model for hysteresis nonlinearity of piezoceramic actuators. *Precision Engineering*, **20**, pp. 99-111.
- Hagglund T. and K. J. Astrom (2002). Revisiting the Ziegler-Nichols Tuning Rules for PI Control. *Asian Journal of Control*, **4**, pp. 364-380.
- Huang, Y. C. and D. Y. Lin (2004). Ultra-Fine Tracking Control on Piezoelectric Actuated Motion Stage Using Piezoelectric Hysteretic Model. *Asian Journal of Control*, **6**, pp.208-216.
- Hwang, C. L. and C. Jan (2003). A Reinforcement Discrete Neuro-Adaptive Control for Unknown Piezoelectric Actuator Systems With Dominant Hysteresis. *IEEE Transactions on Neural Networks*, **14**, pp. 66-78.

- Hwang, C. L., C. Jan and Y. H. Chen (2001). Piezomechanics Using Intelligent Variable-Structure Control. *IEEE Transactions on Industrial Electronics*, **48**, pp. 47-59.
- Ku S. S., U. Pinsopon, S. Cetinkunt and S. Nakajima (2000). Design, Fabrication, and Real-Time Neural Network Control of a Three-Degrees-of-Freedom Nanopositioner. *IEEE/ASME Transactions on Mechatronics*, **5**, pp. 273-280.
- Shen J. C. (2002).  $H^\infty$  Control and Sliding Mode Control of Magnetic Levitation System. *Asian Journal of Control*, **4**, pp. 333-340.
- Tao, G and P. V. Kokotovic (1995). Adaptive Control of Plants with Unknown Hysteresis. *IEEE Transactions on Automatic Control*, **40**, pp. 200-212.
- Utkin V., J. Guldner and J. Shi (1999). *Sliding Mode Control in Electromechanical Systems*. Taylor & Francis, Padstow.
- Xu J. H. (1993). Neural Network Control of a Piezo Tool Positioner. *Proceedings of Canadian Conference on Electrical and Computer Engineering*, pp. 333-336.